

Combined PIV and DGV applied to a pressurized gas turbine combustion facility

C. Willert, C. Hassa, G. Stockhausen, M. Jarius, M. Voges, J. Klinner

Abstract The paper provides an overview of flow field measurements on a pressurized generic combustor that shares typical features of realistic gas turbine combustors. Both Doppler global velocimetry (DGV) and particle image velocimetry (PIV) were applied in parallel to achieve volumetric, three-component velocity data sets of the reacting flow field at pressures of 2 and 10 bars with 700 K pre-heating. Limited optical access to the mixing zone required a combination of PIV and DGV to obtain averaged three-component velocity data from a single viewing direction. The final volume data sets of the time-averaged flow in the mixing zone contain about 40 parallel planes spaced at 2 mm with a spatial resolution of 1.2 x 1.2 mm each. Difficulties encountered in the application of stereoscopic PIV to a simple atmospheric generic combustor illustrate the advantage of the combined PIV-DGV technique. Furthermore current knowledge on solid particle seeding methods required for reactive flow measurements is presented.

1 Introduction

Combustion related research projects are of steadily increased importance at the Institute of Propulsion Technology of DLR. Often these projects are driven by similar motivations, namely to provide experimental data to validate advanced simulation methods which model the extremely complex flows found in modern aero-engine or stationary gas-turbine combustors. To offer a reliable alternative to expensive full-scale rig tests, confidence in CFD results needs to be built not only on basis of validation experiments that capture a single aspect of the flow where the corresponding physical model is tested in isolation. In order to judge the performance of CFD codes in realistic applications, data must also be obtained from facilities that are capable of capturing the rather comprehensive range of effects found inside the combustion chamber in relevant geometries and at higher pressures. Since the complexity and operational cost of a real aero-engine sector combustor prevents the application of advanced optical measurement techniques to fully catch the range of phenomena, compromises must be made such that generic combustors are selected. One of these generic combustors will be described herein.

Many of these generic combustor test rigs are designed to suit a variety of optical diagnostics with special emphasis on planar imaging methods. Aside from the velocity field measurement techniques PIV and DGV, to be described later, a number of spectroscopic techniques are frequently applied: laser induced fluorescence (LIF). Temperature data are acquired using OH-thermometry, CARS (Coherent Anti-stokes Raman Scattering) and SRS (Spontaneous Raman Scattering). Major species concentrations as well as the mixture fraction in the primary zone of the combustor are also measured using SRS (Wehr et al. 2005). PDA (Phase Doppler Anemometry) is used for the measurement of droplet sizes of liquid fueled facilities while LDA (Laser Doppler Anemometry) data augment the whole field measurements with higher precision and statistics. Further information on these techniques and their applications can be found in Behrendt et al. (2000, 2003), Zarzalis et al. (2002), Eggels & Hassa (2005).

With regard to the combustor's velocity field both particle image velocimetry (PIV) and Doppler global velocimetry (DGV) currently are the most suited candidates for efficiently providing data at reasonably high spatial resolutions. Although more precise, single point measurement techniques such as laser Doppler anemometry generally are too costly in order to volumetrically map entire flow fields. Two-component PIV (using a single-camera) has been demonstrated on pressurized combustors (Willert & Jarius, 2002) and now is frequent demand for

C. Willert, C. Hassa, G. Stockhausen, M. Jarius, M. Voges, J. Klinner
Institute of Propulsion Technology, DLR German Aerospace Center, 51170 Koeln, Germany

Correspondence to:
C. Willert, Institute of Propulsion Technology, DLR German Aerospace Center, 51170 Koeln, Germany
E-mail: chris.willert@dlr.de

reactive flow measurements. In parallel, DGV recently has also been successfully qualified for use in reactive flows using a specially designed frequency-stabilized laser (see e.g. Fischer et al., 2000, 2004).

One of the clear advantages of DGV with respect to PIV is that blurring of particle images due to temperature-induced strong gradients of refractive index can be tolerated. However, in order to obtain three-component velocity data with DGV typically four optical access ports are required to achieve at least three light-sheet – camera viewing combinations. Installation of large optical windows with appropriate cooling is not only costly but may also influence the flow under investigation. Other facilities oftentimes impose additional restrictions that make the standard application of DGV unfeasible. On the other hand stereo-PIV may be used in applications without significant optical distortion, such as in combustors operating at atmospheric conditions. As will be described in one of the following sections, even a nearly completely transparent facility is not necessarily well suited for stereoscopic PIV.

For these reasons a combination of DGV with PIV seems very attractive as only two access ports are required: one for the light sheet, the other for the receiving optics (e.g. camera system). While PIV provides the in-plane velocity components, the frequency shifts measured by DGV can be used to estimate the out-of-plane velocity component given knowledge of the PIV components. Boemmels & Roesgen (2002) as well as Wernet (2004) have previously described the underlying principles and have demonstrated it on simple flows using pulsed Nd:YAG lasers thereby providing unsteady 3-C velocity data. The approach used in this investigation only differs by the fact that time-averaged velocity data is produced using DGV in an averaging mode (Willert 2000). Of course this requires a large number of PIV recordings (≥ 100). At this point the non-availability of a suitable double pulsed light source (for PIV) with a sufficiently narrow-bandwidth (for DGV) prohibits a simultaneous application of both techniques at our labs. Rather both methods are applied in succession.

The following sections describe the experimental difficulties in applying stereoscopic PIV in a rather simple facility, followed by an overview of the currently employed seeding methods. The combination of PIV with DGV and results from the technique's application to a pressurized facility concludes the paper.

2

Stereoscopic PIV in a small combustor – A feasibility study

Figure 1 shows an example of a typical small-scale atmospheric combustion chamber for parametric studies of fuel nozzle performance or the investigation of combustion instabilities. The single fuel nozzle is located in the center of the square base area. Three of the four side walls are transparent over the entire height of the combustor (2 mm thick quartz glass); the fourth side consists of a steel plate that supports various diagnostics (temperature sensors, microphone ports) and flame monitoring hardware. In the framework of providing CFD validation data the research program asked for phase-resolved velocity data from the complete volume.

The ample optical access of this combustor makes it especially well suited for a wide variety of optical diagnostics including planar velocimetry (e.g. PIV and DGV). By traversing the light sheet through the volume, the complete (averaged) flow field inside the combustor can be recovered efficiently. Stereoscopic PIV, capable of recovering all velocity components, was chosen for this purpose. A preliminary investigation selected the best suited imaging configuration, three of which will be described next. The configurations are schematically outlined in Figure 2 along with sample PIV recordings that were obtained under ideal conditions, namely, without any window contamination due to seeding deposits.

Configuration 1

In this case the light sheet has a coaxial alignment and is viewed by the cameras from opposing sides in forward scattering (30° off-normal). Along the centerline about two-thirds of the cross-section is visible decreasing to a common area of about one-third the baseline if the light sheet is traversed to either side. Although the signal gain in the PIV recordings due to forward scattering is quite significant (about a factor of 5), a number of undesired artifacts are visible as vertical stripes in the images. One significant stripe is generated by the light sheet as it passes through either surface of the glass window. With increased seeding deposits on the window this scatter will increase up to sensor saturation prohibiting measurements in the proximity of the wall. The reflection of this scatter line can also be observed with a less intensity on the adjacent window. Additional glare is introduced by the vertical pillars supporting the glass windows. This illumination stems from the light scattered from the solid wall onto which the light sheet impinges.

Configuration 2

Here the light sheet has a cross-sectional alignment and is symmetrically viewed by the cameras at angles of 45° . One of the cameras takes advantage of the forward scatter gain while the other operates in backward scatter with

signal levels similar to a normal viewing (90°) setup. The light sheet passes straight through the facility in order to reduce flare caused by a solid wall. This arrangement was favored because the swirling flow exiting the nozzle could be captured instantaneously. Just as in the previous case, significant stray light is scattered where the light sheet passes through the windows. The also signal increases due to forward scattering. The stray light is also reflected by the bottom face of the combustor. Use of an additional mirror to increase signal to the back-scatter camera did not result in any noticeable improvements.

Configuration 3

This configuration combines a classical light-sheet normal viewing arrangement with a 45° off-axis view. The light sheet also passes straight through the facility keeping possible flare to a minimum. The full axial length of the combustor is visible to the normal view camera while the oblique view is limited by the lid.

Compared to the previously described arrangements this setup exhibits the least amount of scattered light for either camera view and therefore was chosen for production measurements. Nonetheless window contamination due to seeding deposits during operation results in quite significant light scatter after about 2 minutes of continuous supply of particles. Also the solid wall is partially reflective and causes additional signal degradation. In effect, a fourth (!) transparent side on the combustor would be required to maintain good signal levels.

The previous configurations clearly illustrate the importance of proper treatment of light scatter in confined arrangements. In effect the window-normal imaging setups produce the best results, partially also because reflections reach a minimum in when light passes at normal angles through a window. Based on this observation methods relying only on window-normal imaging should be preferred to oblique views. The combination of two-component PIV with DGV to retrieve the out-of-plane component fulfills these criteria.

3

Measurement techniques

PIV technique

An overview on the application of PIV in reactive flows is already given in Willert & Jarius (2002) such that only the most important aspects shall be repeated here. The hardware shares components that are commonly used in PIV applications: a double-pulse, frequency pulsed Nd:YAG laser with 120mJ/pulse, light sheet forming optics and a thermo-electrically cooled mega-pixel CCD camera (1280x1024 pixel @ 12bit/pixel) capable of capturing two image frames within several microseconds. The influence of flame-radiation on the CCD was reduced by placing a laser-line filter (532 nm @ 5nm FWHM) in front of the 55 mm objective lens. Additional camera shuttering as suggested in Willert & Jarius (2002) was not required due to the rather moderate flame luminosity inside the combustion facilities described here.

DGV technique

The DGV technique is based on the measurement of the frequency shift associated with the movement of the particles with the flow (Doppler shift). It differs from PIV in that individual particles need not be resolved. Rather the Doppler frequency shift is inferred from an intensity-based measurement of the frequency-dependent transmission of a molecular (or atomic) absorption cell. The underlying principles are described exhaustively in literature (e.g. Elliot & Beutner, 1999; Samimy & Wernet, 2000; Willert, 2005). It should be noted that the DGV systems at DLR are mostly operated in a time-averaging mode using CW-lasers and on-chip image integration (Roehle, 1998; Roehle et al, 2000). The DGV system used in the present application relies on a specifically designed Nd:YAG laser system that is capable of producing single-frequency laser pulses at 1 kHz at a mean power of 1.5 W and wavelength of 532 nm. The resonator/amplifier configuration is designed to produce rather long pulses of 300 ns – compared to 5-20 ns for standard Nd:YAG pulsed lasers – and therefore exhibits a narrow line-width in the 5 MHz range which is an essential requirement for reliable DGV measurements. Although the system was operated in a time-averaging mode, a pulsed laser was chosen in place of a CW laser, because the pulsed illumination in conjunction with appropriate camera shuttering achieves a much higher signal-to-noise ratio in the presence of flame luminosity. Further details on this system and related applications are given in Fischer et al. (2000, 2004).

Since the laser system is very susceptible to noise or vibration it was placed in a separate room located about 10 m away from the combustor facility. The laser light was delivered to the scanning light sheet systems by 15 m long fibers with a core diameter of 200 μm . It should be noted here that fiber-based laser-light delivery is not possible with higher power Nd:YAG lasers.

Seeding technique

Proper aerosol seeding of the flow remains one of the most challenging issues in planar velocimetry in general and is even more demanding in reactive flows as solid particles with high vaporization¹ temperatures must be used. In practice metal oxides such as alumina (Al_2O_3), silica (SiO_2), titania (TiO_2) or zirconia (ZrO_2) are frequently chosen. The challenging aspect of solid particle seeding is the dispersion and delivery of the powder to the test section, while ensuring that the generally agglomerated powders are properly broken down to their primary grain size. This dispersion can be achieved very efficiently through by careful adjustment of the polarity in aqueous or ethanol solutions of the powder (Wernet & Wernet, 1994). However this approach is not particularly suited to combustion environments because the presence of evaporated water or ethanol will change the reactive chemistry.

In the current application a flow seeding based on fluidized bed was chosen. The seeding device consists of a vertical pipe (700 mm length, 100 mm diameter) with an air supply at its bottom that is used to aerate the powder. Through proper adjustment of the mean air flow only smaller particles are carried toward the exit orifice at the top of the seeder. There a sonic flow nozzle is intended to break up larger clusters due the high strain rate. From there the connection to the delivery system is kept as short as possible to prevent agglomeration of seeding prior to entry into the facility. A by-pass system maintains mass flow rates into the facility while seeding is disabled. This allows introduction of seeding only during data acquisition phases which reduces the overall window contamination and thereby increases the total operational time of the facility before window cleaning is required. In the previously described atmospheric combustor the lack of window cooling air film limited the continuous seeding period to about 2 minutes before the light scattered by seed material on the windows saturated the sensor (Fig. 3). With window film cooling as in the pressurized facility much longer measurement times were feasible.

The seeding material itself consisted of alumina particles (Al_2O_3) with a size distribution of 0.2 to 1 μm . This material exhibits rather strong hygroscopic behavior which resulted in increased agglomeration. Therefore the powders were heated to remove residual moisture prior to filling the seeder. Whenever possible, pressurized dry nitrogen was used in place of pressurized air to operate the seeding device. With regard to seeding quantities both DGV and PIV required similar amounts: the mass flow through the seeder was on the order of 1-2 g/s in the pressurized facility. Further information on different powdered materials suitable for high-temperature flow seeding is given in the appendix.

Combined DGV and PIV

The previously described measurement techniques were applied in succession rather than simultaneously because different illumination and imaging hardware was involved. For each imaged plane 100 PIV recordings were acquired at about 3 Hz frame rate (2 μs pulse separation) from which the mean in-plane velocity was calculated. Subsequently time-averaged, single-component DGV recordings were acquired for the same slices through the volume. Each DGV recording represents the integrated intensity of about 5000 individual pulses from the pulsed laser system.

Samples of the 2-C PIV velocity and DGV frequency shift data are shown in Fig. 3. The PIV image data was first band-pass filtered to enhance particle image contrast and then processed with interrogation areas of 32×32 pixels ($\cong 2.5 \times 2.5 \text{ mm}^2$) at 50% overlap using a first-order, multiple-pass correlation algorithm (e.g. without adaptive image deformation). Validation was performed by application of a magnitude threshold and neighborhood comparison operator. The averaged displacement data was validated a second time by requiring a validation rate of at least 20% at each sample point.

The DGV frequency shift images were obtained using the standard DGV processing steps, that is, background image subtraction, calculation of the intensity ratio, normalization with a flat field image and application of the intensity-to-frequency look-up table. The camera image intensifiers and the fiber imaging bundle used for the collection of image introduced a grainy structure in the images such that spatial averaging (low-pass filtering) with a 5×5 pixel kernel was applied.

The combination of the two distinct data sets is accomplished by taking the imaging geometry (viewing angles and distances) into account as shown in Fig. 4. While PIV essentially records the in-plane velocity components, DGV recovers the projection of the velocity vector onto the difference vector between light-sheet and observation vectors (σ - l). As the DGV-component is not co-planar with the plane spanned by the two PIV components, the three (orthogonal) velocity components can be determined by a straight-forward matrix inversion. In practice the denser DGV data is locally averaged corresponding to the coarser PIV data grid.

¹ A melted particle would still be visible in a flame, so the vaporization temperature is the relevant figure.

4

DGV-PIV on a pressurized combustor

4.1 Facility

Within the EC-funded project MOLECULES (MODelling of Low Emissions Combustors using Large Eddy Simulations) a generic combustor was designed to simulate typical features of realistic combustors (Fig. 5). This so-called *single sector combustor* (SSC) has a square cross-section and features a gaseous fuel burner whose aerodynamic characteristics match a generic diffusion burner for spray combustion. The natural gas fuel is fed into the swirl channels through an array of tubes ending in 4 ports. The swirl channel lacks a diffuser and ends in a straight section thus providing well defined boundary conditions at the entry plane to the combustion chamber. A rather strong air flow swirl angle of 60° was chosen to achieve a stable recirculation zone within the combustor without fuel swirl. The mixing zone down-stream of the burner is initiated by several cross-flow air jets which face each other. The air mass flow through the side jets was separately controlled to ensure the right amount of collision of the jets. Two operating conditions at 2 and 10 bars with 700K pre-heating were chosen to investigate the influence of changing kinetic rates on combustion processes: A variety of optical measurements was applied to collect comprehensive validation dataset.

The facility has good optical access in two important regions within the combustor. The primary zone immediately above the swirl burner is optically accessible from three sides with windows spanning the entire cross-section of the combustor. Further down-stream, access to the mixing zone and its impinging secondary air jets is achieved by two opposing windows. To nonetheless permit classical light-sheet normal imaging configurations in the mixing area two more small windows were placed in the exit plane of the combustor parallel to the slotted sonic nozzle. These windows can be used to introduce a light sheet as described in the following section. Alternatively cross-sectional views of facility can be obtained as in the case of three-component DGV measurements of the primary zone (Stockhausen et al., 2004). Except for the exit port windows all windows consist of a thick pressure window and an inner liner window. Air film cooling on the liner windows prevents heat damage as well as the build-up of seeding. More detailed information on the facility itself is given by Eggels and Hassa (2005).

4.2

Measurement results

The combined PIV-DGV technique was chosen for the investigation of the mixing zone in the previously described single sector combustor rig at pressures of 2 and 10 bar. The aim was to obtain a near complete volumetric map of three-component velocity data in this area which has optical access through two windows facing each other along with narrow windows on the exit plane (Figures 4, 5). This arrangement limited the application of stereoscopic PIV to map the mixing jet area near the wall. A more detailed map could only be obtained through a combination of both DGV and PIV with the light sheet introduced through the top window. In this arrangement the entire combustor facility could be traversed in all three coordinates to allow a convenient volumetric mapping of the combustor's flow field.

The final volumetric data sets for 2 and 10 bar are given in Fig. 7 and respectively consist of 41 and 39 individual planes spaced at 2 mm increments. The in-plane spatial resolution is about $1.2 \times 1.2 \text{ mm}^2$. Fig. 8 presents two slices through these data sets and clearly shows the blocking influence of the mixing jets within the secondary zone. Comparison of the respective 2 and 10 bar pictures shows little differences, which is reassuring, since the jet large scale mixing in a uniform cross-flow should not change such that only the different velocity distribution of the primary zone has an influence. Here only the axial position of the acceleration due to combustion is different because of the different kinetic rates at 2 and 10 bar, the heat release being nearly completed at the entrance plane of the jets. The overall primary zone momentum thus not differing by much, the changed form of the primary zone velocity profiles shows up most clearly in the somewhat wider central recirculation zone on the axial velocity distribution at $z = 78 \text{ mm}$ in Fig. 8. It also shows that the spreading and collision of the large central jets effectively ends the recirculation at the mixing jet plane marked in Fig. 7, which is one of their intended uses in order to limit the primary zone residence time.

The influence of the collision of the central mixing jets on the amount of secondary air transported upstream is also of interest, since it can be used to modify the primary zone equivalence ratio. However its prediction is rather difficult since it depends on the turbulent jet mixing as well as on the interaction with the swirling flow both exhibiting coherent structures and unsteady behavior. This is one of the reasons why LES as a method to compute unsteady flows is also attractive for the computation of an operating condition that is otherwise in steady state.

Visual comparison of the two data sets already also reveals that the 10 bar data contains more noise than the 2 bar data which has two reasons. First of all the mass flow rate from 2 to 10 bar increased a factor of five while seeding

rates could not be raised in a similar fashion. Secondly refractive index variations increase with increasing pressure leading to strong particle image blurring. Overall the measurement uncertainty is on the order of 3 m/s (0.1 pixel) for a single PIV recording, or 0.3 m/s for the statistical average of 100 images. The DGV measurement uncertainty is on the order of 5 MHz based on the noise in frequency shift images. This translates to a velocity uncertainty of approximately 1.5 m/s.

5

Summarizing remarks

Although the previously described measurements on fired combustors yielded very reasonable results, the path toward reaching this goal involved a number of set-backs. A full description of the methods and approaches involved various problem solutions are beyond the scope of this article. In summary it should however be clear that the application of both PIV and DGV methods in combustion facilities is still undergoing considerable development steps.

One recent improvement on the side of DGV, for instance, was achieved through closer investigation of background scene illumination due to light scattered by the particles. This additional signal results in a loss of contrast in the frequency shift images and biases the measured velocity toward zero (Fig. 9). Through appropriate treatment of the acquired data prior to processing, the contrast in the frequency shift images could be restored (Stockhausen et al. 2004).

Further improvements also are to be expected with regard to laser technology: a laser system based on a solid-state pumped thin-disk resonator concept has been acquired and already has been shown to operate in a frequency stabilized mode. Its continuous single-mode output power reaches 5 W at 514 nm with a line width of approximately 10 MHz. A tuning range in excess of 50 GHz now allows the use of iodine absorption lines that were previously out of reach for argon ion lasers. With regard to energy and water consumption this system merely requires power from a standard wall socket and is much easier to transport – an important advantage given the frequent out-of-house applications of DGV. Compared to the argon ion laser this system is simpler to stabilize.

Regardless of their future development none of the planar velocimetry techniques (e.g. PIV and DGV) will be able to surpass single point techniques such as LDA or LTA (laser transit anemometry, or laser laser-2-focus velocimetry, L2F) with regard to measurement precision. The strategy followed at the Institute of Propulsion Technology is to use PIV or DGV to capture a global (more qualitative) overview coupled with point-wise techniques (PDA, LDA, LTA) for precise measurements with improved statistics. The combination of planar velocimetry with spectroscopic techniques is of increased importance as it allows to establish, for instance, the correspondence between heat release zones and an oscillating flow field (Fischer et al. 2004).

Acknowledgements

This work is part of the research project *MOLECULES* and has been funded by the European Community under the 'Competitive and Sustainable Growth' Programme (1998-2002), Contract N°: G4RD-CT 2000-00402. The support is gratefully acknowledged. Special thanks are expressed for the excellent support of W. Quade on the single sector combustor (SSC). Also we would like to acknowledge the efforts by R. Borath of DLR's Institute of Materials Research for providing the micrographs of the seeding materials.

References

- Behrendt T, Heinze J, Hassa C, (2000)** Optical measurements of the reacting two-phase flow in a realistic gas turbine combustor at elevated pressures, *ILASS-Europe, Darmstadt, 11-13 September*
- Behrendt T, Heinze J, Hassa C (2003)** Experimental investigation of a new LPP injector concept for aero engines at elevated pressures, *ASME-GT-38444*
- Boemmel R, Roesgen T (2002)** Planar three-component velocimetry with DGV and PIV - A combined measurement technique. Proc: *10th Intl Symp Flow Visualization (ISFV10)*, Kyoto (Japan), 25-29 August, vol. 1, page F0108.
- Elliot GS, Beutner TJ (1999)** Molecular filter based planar Doppler velocimetry. *Prog. Aero Sci* 35:799-845
- Eggels RLGM, Hassa C (2005)** Modelling of the flow field within a generic aero-engine combustor. *41st AIAA/ASME/SAE/ASEE Joint Propulsion Conference*, Tuscon, AZ, 10-13 July, AIAA-2005-3970.

- Fischer M, Heinze J., Matthias K, Roehle I** (2000) Doppler global velocimetry in flames using a newly developed, frequency stabilized, tunable, long pulse Nd:YAG laser. Proc: 10th Intl. Symp. on Applications of Laser Techniques to Fluid Mechanics, Lisbon (Portugal), 10-13 July
- Fischer M, Stockhausen G, Heinze J, Seifert M, Müller M, Schodl R.** (2004) Development of Doppler Global Velocimetry (DGV) measurement devices and combined application of DGV and OH* chemiluminescence imaging to gas turbine combustor. Proc: 12th Intl. Symp. on Applications of Laser Techniques to Fluid Mechanics, Lisbon (Portugal), 12–15 July
- Roehle I** (1998) Doppler global velocimetry. *Lecture Series 1998-06: Advanced Measurement Techniques*, von Karman Institute of Fluid Dynamics, Brussels
- Roehle I, Schodl R, Voigt P, Willert C** (2000) Recent developments and applications of quantitative laser light sheet measuring techniques in turbomachinery components. *Meas Sci Technol* 11:1023–1035
- Samimy M, Wernet MP** (2000) Review of planar multiple-component velocimetry in high-speed flows. *AIAA Journal* 38:553-574
- Stockhausen G, Fischer M, Heinze J, Mueller M** (2004) Anwendung von DGV in heißen Brennkammern. Proc: 12. GALA Fachtagung Lasermethoden in der Strömungsmesstechnik, Karlsruhe (Germany), 7-9. Sept. 2004
- Wehr L, Kutne P, Meier W, Becker J** (2005) 1D Single-Pulse Raman Measurements of Temperature and Mixture Fraction in a Gas Turbine Model Combustor at Elevated Pressure. *European Combustion Meeting*, Brussels.
- Wernet P** (2004) Planar particle imaging Doppler velocimetry: a hybrid PIV/DGV technique for three-component velocity measurements. *Meas. Sci. Technol.* 15: 2011-2028
- Wernet JH, Wernet MP** (1994) Stabilized alumina/ethanol colloidal dispersion for seeding high temperature air flows. *ASME Symp. on Laser Anemometry: Advances and Applications*, Lake Tahoe, NV, 19-23 June
- Willert C** (2000) Feasibility study for the combination of PIV with Doppler global velocimetry (DGV) *Pivnet T5/ERCOTAC SIG 32, 2nd Workshop on PIV*, Lisbon, 7-8 July 2000
- Willert C** (2005) Doppler global velocimetry – Fundamentals, implementation and selected applications, VKI-Lecture Series, *Advanced Measurement Techniques for Supersonic Flows*, February 28 – March 3.
- Willert C, Jarius M** (2002) Planar flow field measurements in atmospheric and pressurized combustion chambers, *Exp.Fluids* 33: 931-939
- Zarzalís N, Ripplinger T, Hohmann S, Hettel M, Merkle K, Leuckel W, Klose G, Meier R, Koch R, Wittig S, Carl M, Behrendt T, Hassa C, Meier U, Lücknerath R, Stricker W,** (2002) Low-NO_x Combustor Development pursued within the scope of the Engine 3E German national research program in a cooperative effort among engine Manufacturer MTU, University of Karlsruhe and DLR German Aerospace Research Center, *Aerospace Science and Technology*, 6: 531-544



Figure 1: Generic combustor used for optical diagnostics of the reactive flow.

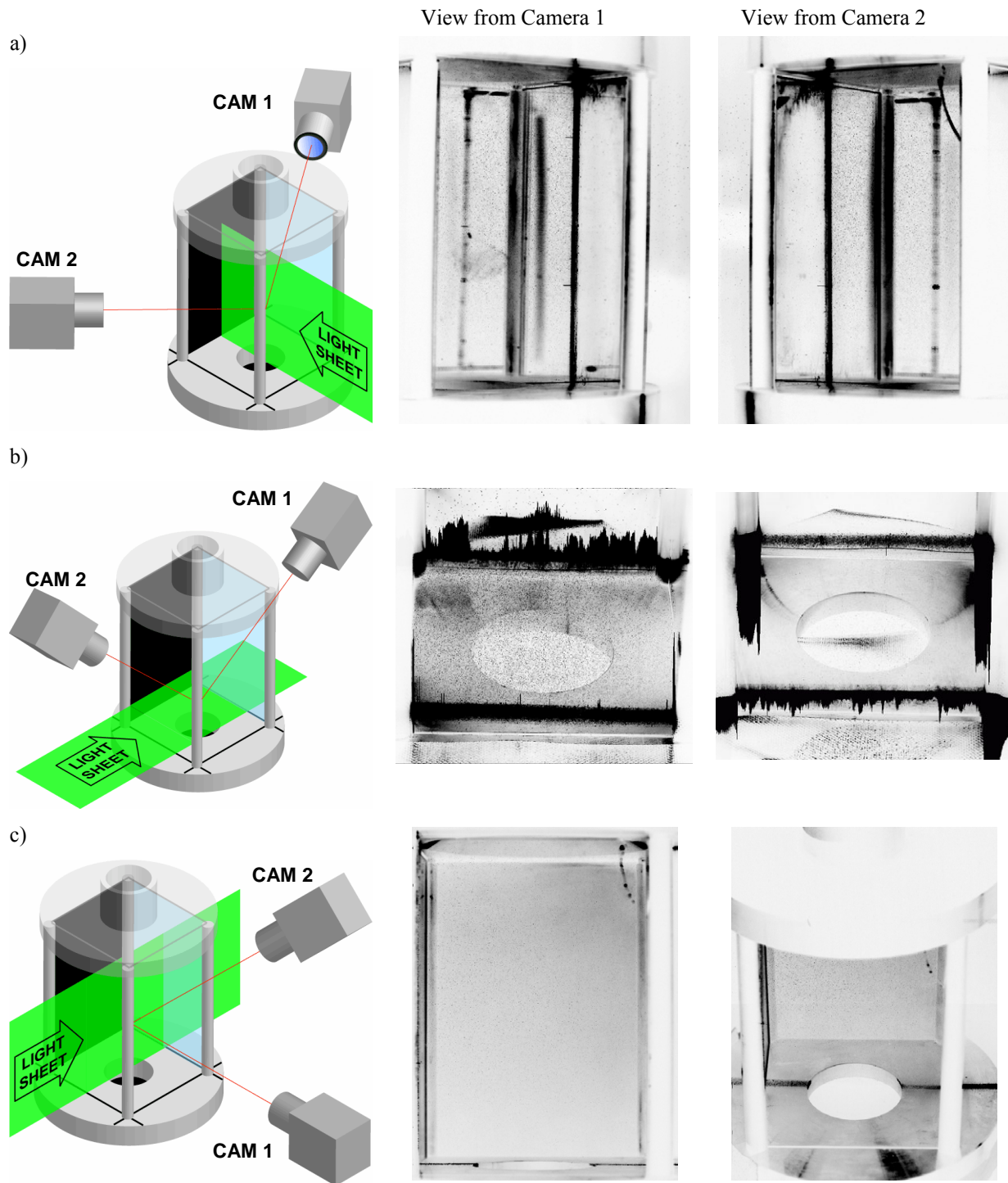


Figure 2: Three possible stereoscopic PIV imaging configurations capable of recovering volume-resolved three-component velocity data. Sample PIV recordings by the cameras illustrate problems due to reflections. The PIV recordings are intensity-inverted for clarity with black regions indicating significant light scatter.

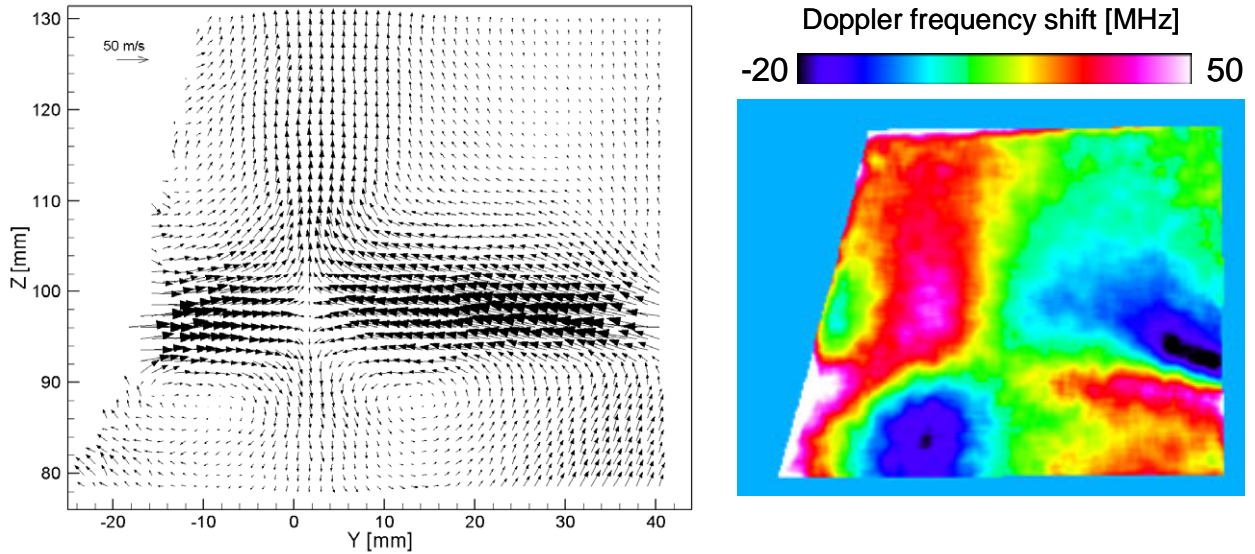


Figure 3: Average of 100 PIV recordings (left) and corresponding image of frequency shifts obtained by DGV in the secondary zone at 2 bar in the facility shown in Figure 6.

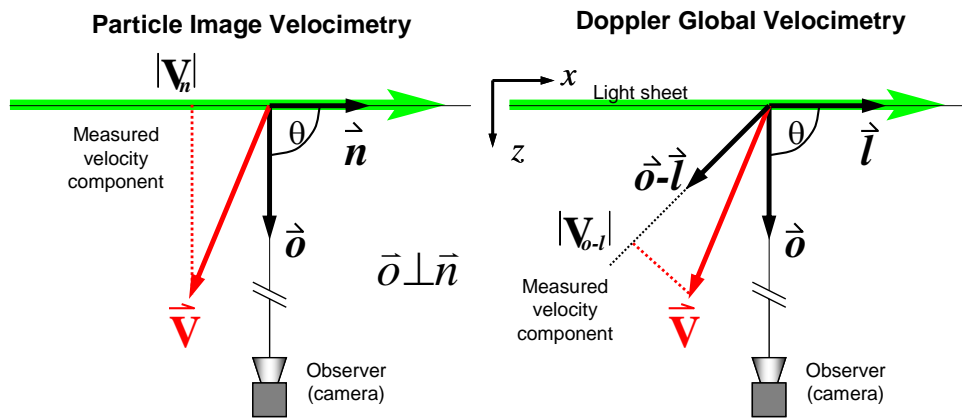


Figure 4: Combination of DGV with PIV permits three-component velocity measurements using a single light sheet observed from a single optical viewing direction.

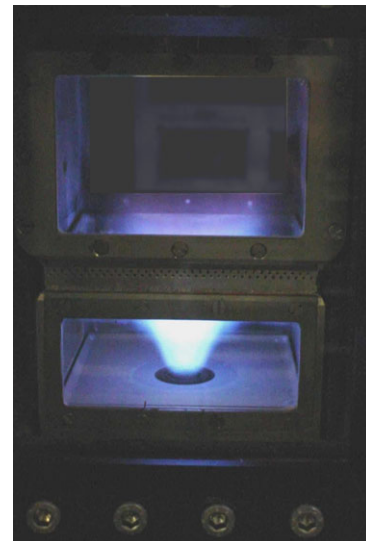
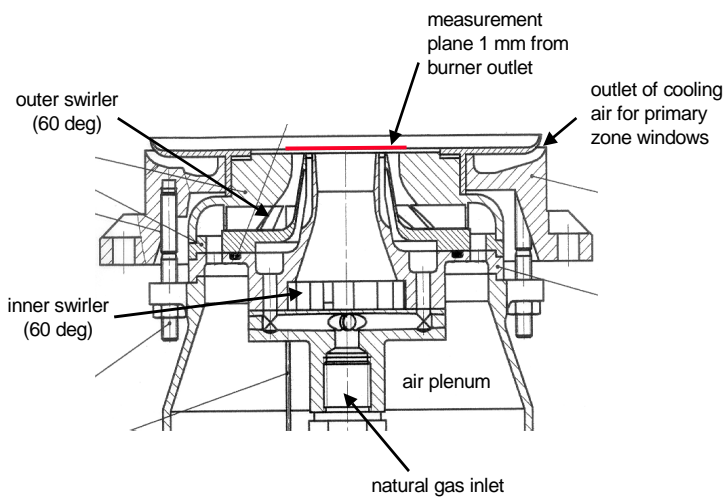
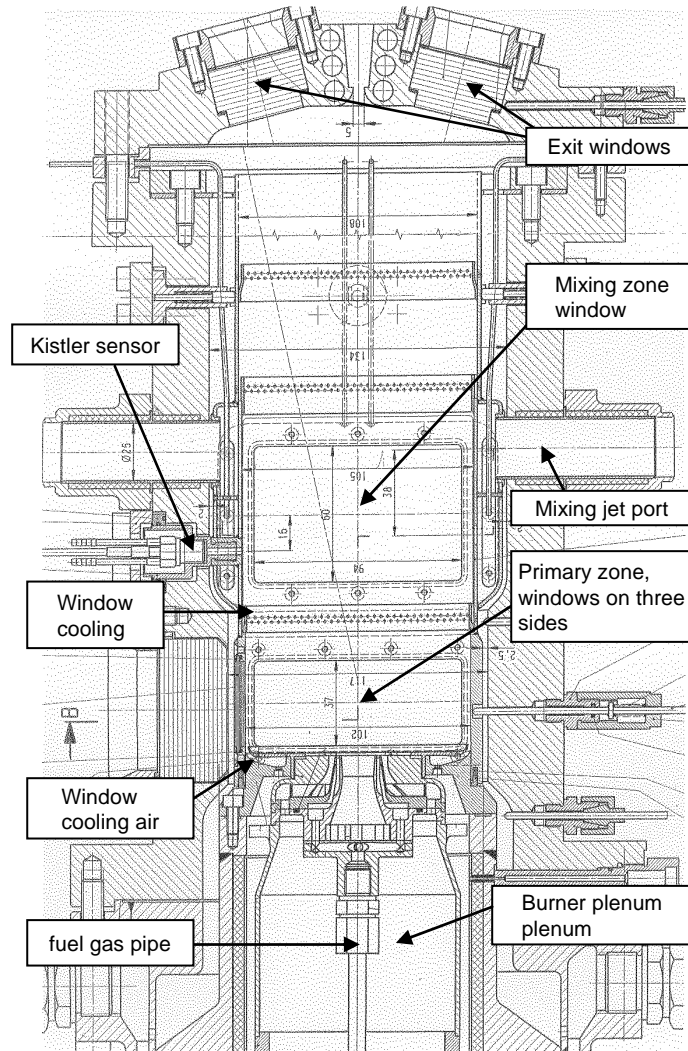


Figure 5: Generic combustor with optical access to primary and mixing zones (top). Bottom left: longitudinal sectional of the co-rotating swirl flow burner. Bottom right: photograph of the reacting flow at 4 bar and pre-heating of 700 K.

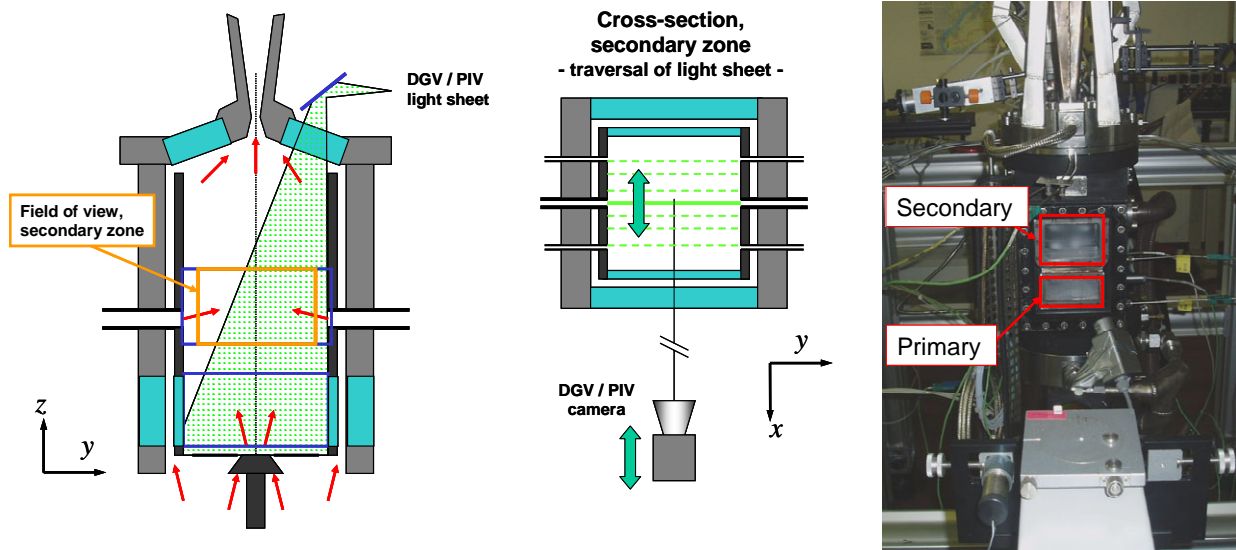


Figure 6: Application of combined DGV and PIV to the pressurized single-sector combustor.

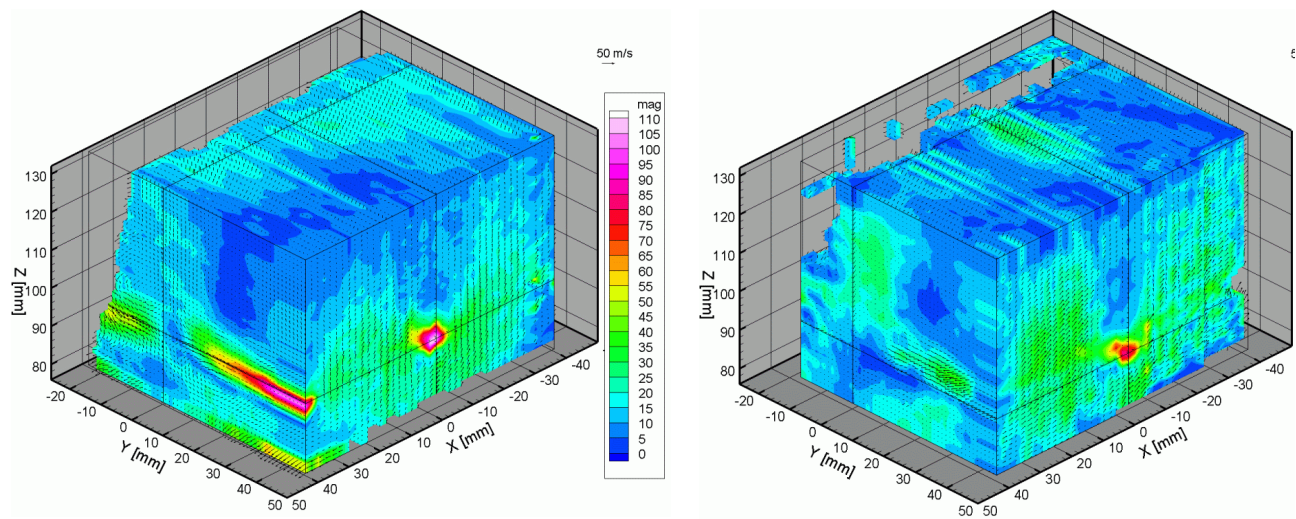


Figure 7: Volume data set obtained for the reacting flow in the mixing zone of the combustor shown in Figure 4 operating at 2 bar (left) and 10 bar (right). Data was obtained through the combination of DGV with PIV and has spatial resolution of $2 \times 1.2 \times 1.2 \text{ mm}^3$. Color-coding represents velocity magnitude. The swirl nozzle coincides with the origin of the coordinate system.

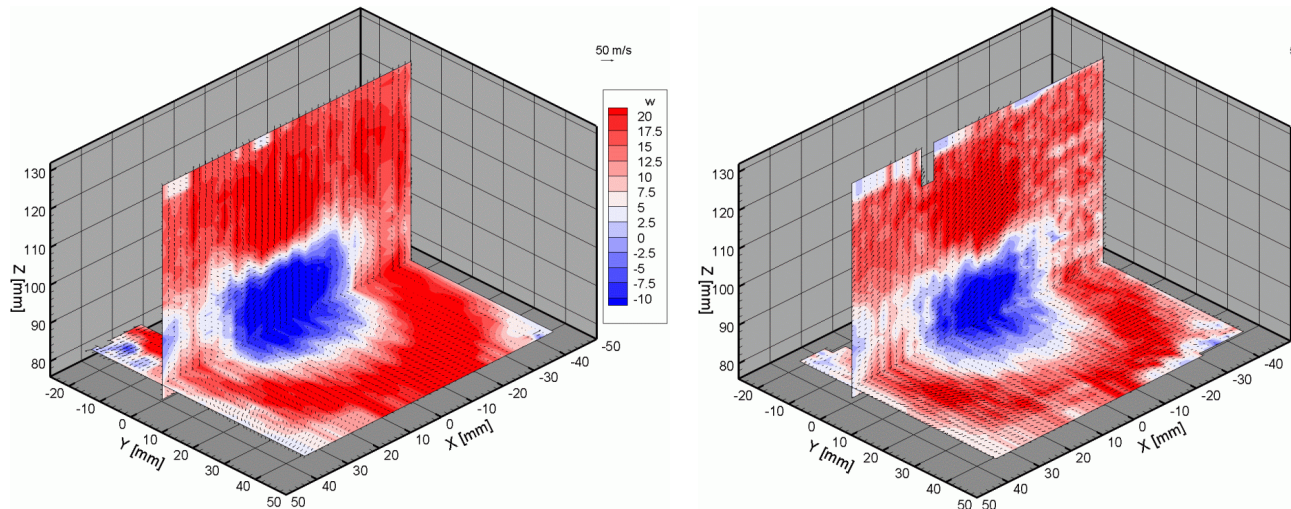


Figure 8: Selected slices through the volume data sets of Figure 7. Color-coding reflects the stream-wise velocity component v_z .

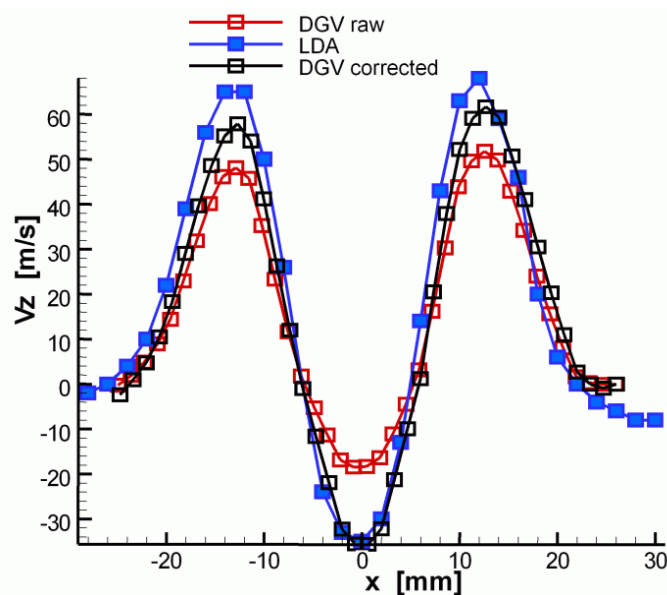


Figure 9: Comparison between LDA and DGV measurements obtained in the primary section of the single sector combustor (from Stockhausen *et al.* 2004).

Appendix – An overview of commonly used solid particle seeding materials

In the previously described application seeding was provided by a generator containing a fluidized bed of alumina particles (Al_2O_3). Operation of the seeder was not always reproducible which in part could be attributed to moisture in the carrier air stream. Although the manufacturer had specified a mean particle size in the $0.8 \mu\text{m}$ range, scanning electron microscopy (SEM) of the particles revealed the presence of a significant number of very small particles in the $100\text{-}300\text{nm}$ range (Figure A1). Particles of this size have very low light scattering (Rayleigh scattering) and are considered to be unsuitable for PIV. It is believed that only a fraction of the particles are resolved by the PIV camera while the bulk of the material adds to a mean background intensity and faster window contamination.

These observations prompted a search for more adequate seeding materials that offer a narrow size distribution in the $1 \mu\text{m}$ range. A few examples obtained during this search are shown in the following SEM images. Titania (TiO_2)

particles are used rather frequently in velocimetry (Figure A2). However they are generally not available with primary sizes suitable for PIV because their primary use for color enhancement demands sizes at half the visible wavelength, that is, below 400 nm. The loss of signal observed inside reactive flows can be attributed to the break-up of larger clusters during the rapid thermal expansion in the reaction zone. Silicon dioxide (SiO_2) particles are shown in Figure A3 and are available as ground material or as spheres. Although more expensive than poly-disperse particles, the spherical mono-disperse particles hold the biggest promise in regard to optimizing the trade-off between facility contamination and signal yield. This was confirmed by preliminary atmospheric tests with this material. Other materials to be tested are made of porous silica with specific weights as low as 0.1 and expected excellent aerodynamic properties.

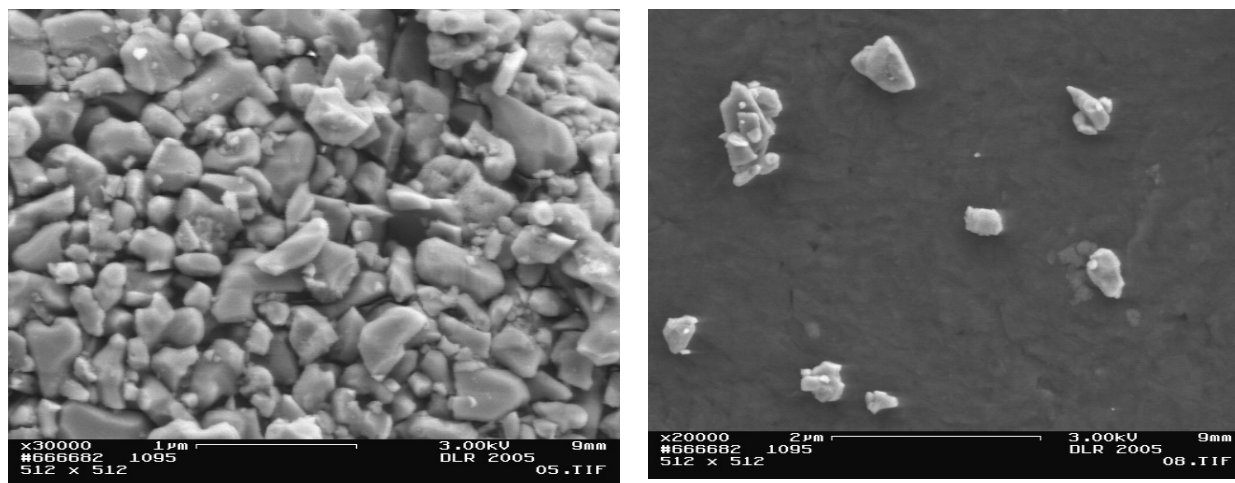


Figure A1: Micrographs of alumina particles (Al_2O_3), densely packed (left) and captured downstream of a flow seeding device (right). These were used for the previously described measurements.

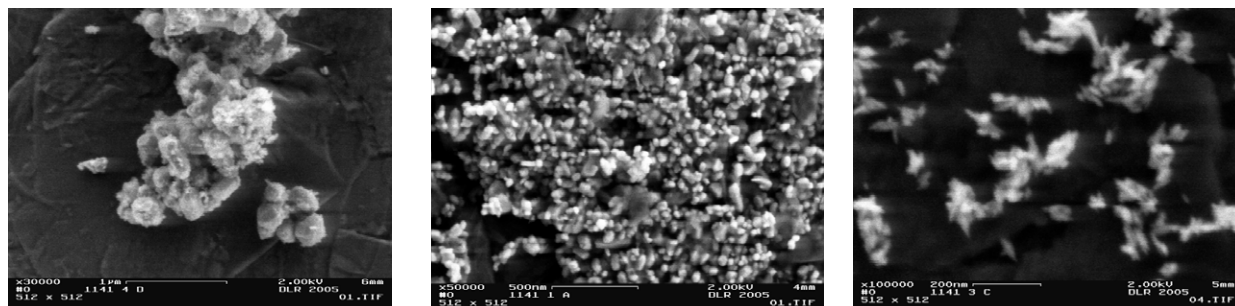


Figure A2: Micrographs of various titania (TiO_2) particles. Peak in size distribution: 410 nm (left), 50 nm (middle), 14 nm (right).

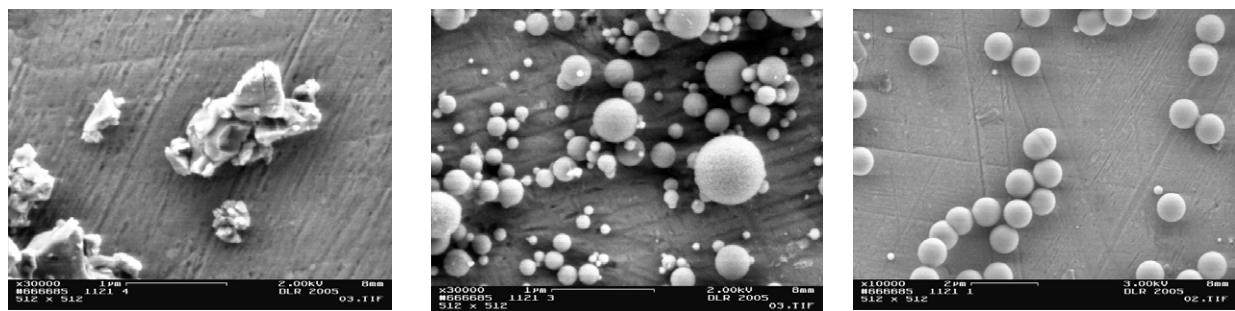


Figure A3: Micrographs of various silica (SiO_2) particles: ground silica (left), poly-disperse spherical (middle) and 800 nm mono-disperse spherical (right).